

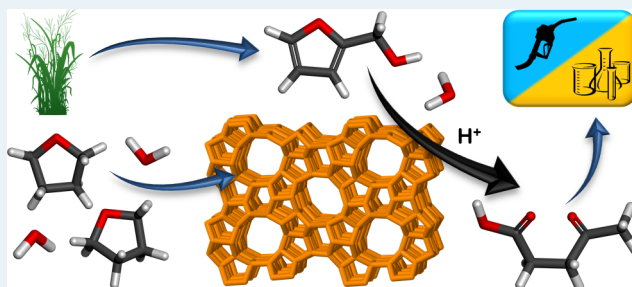
Selective Production of Levulinic Acid from Furfuryl Alcohol in THF Solvent Systems over H-ZSM-5

Max A. Mellmer,^{†,‡} Jean Marcel R. Gallo,^{†,§} David Martin Alonso,[†] and James A. Dumesic^{*,†,‡}[†]Department of Chemical and Biological Engineering, University of Wisconsin–Madison, Madison, Wisconsin 53706, United States[‡]DOE Great Lakes Bioenergy Research Center, University of Wisconsin–Madison, Madison, Wisconsin 53706, United States[§]Department of Chemistry, Federal University of São Carlos, São Carlos, SP 13565-905, Brazil

Supporting Information

ABSTRACT: Furfuryl alcohol in high concentrations (1 M) was hydrolyzed to levulinic acid in high yields (>70%) using H-ZSM-5 zeolite as the catalyst in monophasic tetrahydrofuran (THF)–water solvent systems. Reaction kinetics studies using H-ZSM-5 were carried out, and combined with results obtained for other Brønsted acid catalysts, we suggest that the structural properties of H-ZSM-5, in conjunction with increased reaction performance using the polar aprotic solvent THF, are effective for furfuryl alcohol hydrolysis to levulinic acid while inhibiting furfuryl alcohol polymerization reactions. In addition, on the basis of results obtained for a wide range of THF–H₂O solvent systems (19:1–1:2 w/w), we suggest that the hydrophobic nature of H-ZSM-5 alters the internal solvent microenvironment within the zeolite framework, allowing for high levulinic acid yields, even at low THF solvent concentrations (e.g., 1:2 THF–H₂O w/w).

KEYWORDS: biomass conversion, heterogeneous catalysis, solvent effects, furfuryl alcohol, levulinic acid, ZSM-5

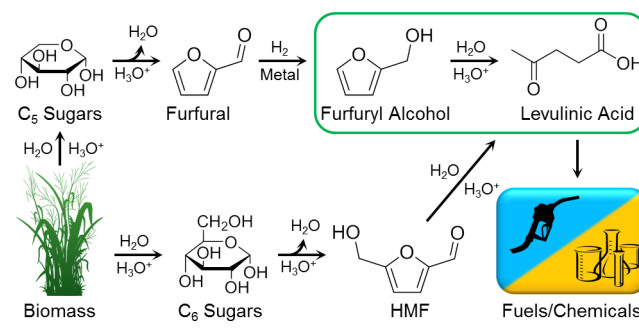


INTRODUCTION

Biomass is an indispensable resource in the quest for an environmentally sustainable source of organic carbon for the future. Analogous with the petrochemical industry, biomass can be converted into a range of versatile chemical building blocks, which can then be subsequently upgraded to compounds suitable to either supplement or replace of our current supply of petroleum-derived chemicals and fuels. One such building block is levulinic acid, which has been deemed a top value-added chemical from biomass because levulinic acid is a precursor to a broad range of organic compounds that address a number of large-volume chemical markets.^{1,2} For example, levulinic acid can be employed in the production of chemicals such as diphenolic acid and δ -aminolevulinic acid³ as well as fuels, such as methyltetrahydrofuran,⁴ levulinate esters,^{5,6} and γ -valerolactone.^{7,8}

Levulinic acid can be produced from the cellulose fraction (C₆ sugars) of lignocellulosic biomass in high yields through a series of acid-catalyzed reactions, passing through the platform molecule hydroxymethylfurfural, as displayed in Scheme 1;^{9,10} however, the use of cellulose for the production of chemicals competes with the well-established bioethanol process.¹¹ Hemicellulose (C₅ sugars) can also be used to target the production of levulinic acid,¹² as shown in Scheme 1. This conversion is achieved through acid-catalyzed dehydration of xylose to form furfural, followed by metal-catalyzed reduction of furfural to furfuryl alcohol, and completed by Brønsted acid-

Scheme 1. Levulinic Acid Production Pathways from Biomass



catalyzed hydrolysis of furfuryl alcohol to levulinic acid. Notably, the conversion furfuryl alcohol to levulinic acid is of fundamental importance because it is one of the few reactions that integrate glucose and xylose reaction pathways,¹³ associating xylose with the well-developed chemistry of cellulose-derived compounds.

One of the major challenges of producing levulinic acid from hemicellulose is the high reactivity of acid-catalyzed polymerization of furfuryl alcohol into unwanted degradation products

Received: February 9, 2015

Revised: April 20, 2015

Published: April 23, 2015

(i.e., humins), resulting in low product selectivities for production of levulinic acid. For example, levulinic acid yields of ~30% are achieved in acidic aqueous medium in a batch system at modest furfuryl alcohol concentrations (0.1 M).¹² Furthermore, furfuryl alcohol hydrolysis¹⁴ as well as furfuryl alcohol polymerization¹⁵ in aqueous acidic solution is mechanistically complex. Thus, furfuryl alcohol conversion into levulinic acid is limited to few scientific papers.

To minimize polymerization problems, the conversion of furfuryl alcohol is usually carried out at low furfuryl alcohol concentration. For instance, Gürbüz et al. developed a processing strategy implementing biphasic reaction systems with alkylphenol solvents.¹² Because of the high partition of furfuryl alcohol to the organic phase, low furfuryl alcohol concentrations were maintained in the acidic aqueous phase, decreasing the rate of the polymerization reactions. However, these biphasic systems required semibatch operation and mineral acid catalysts to achieve high levulinic acid yields (~70%) at high furfuryl alcohol concentrations (1 M). Similarly, using semibatch operation, Lange et al.¹⁶ performed the conversion of furfuryl alcohol in alcohol solvents, producing levulinate esters at high yields; however, when levulinic acid is the desired product, a subsequent levulinate ester hydrolysis step is required.

For the effective conversion of furfuryl alcohol to levulinic acid, it is necessary to find alternative catalysts and processes that allow the production of levulinic acid in high yields starting with furfuryl alcohol solutions in high concentrations. Herein, we report high levulinic acid yields (>70%) with up to 1 M furfuryl alcohol concentrations using monophasic tetrahydrofuran (THF) solvent systems over H-ZSM-5 catalyst. Furthermore, we compare the selectivity trends of H-ZSM-5 with other zeolites, which have previously shown good performance for other biomass conversion reactions, and we explore the effects of varying the SiO₂/Al₂O₃ ratio of H-ZSM-5 on furfuryl alcohol conversion.

■ EXPERIMENTAL DETAILS

Catalyst Preparation. ZSM-5 (Zeolyst; CBV 2314, CBV 5524G, CBV 8014; SiO₂/Al₂O₃ = 23, 50, 80, respectively), Mordenite (Zeolyst; CBV 21A; SiO₂/Al₂O₃ = 20), and Zeolite Beta (Zeolyst; CP814E*; SiO₂/Al₂O₃ = 25) were purchased in the ammonium form and converted to the proton form by calcination in air for 5 h at 823 K (1 K min⁻¹). Ferrierite (Tosoh; HSZ-720 KOA; SiO₂/Al₂O₃ = 18) was purchased in the potassium form, ion-exchanged with ammonium nitrate (1 M, 343 K, 4 h, three times), and converted to the proton form by calcination in air for 5 h at 823 K (1 K min⁻¹). Amberlyst 70 (The Dow Chemical Company) was washed, dried, and crushed before use. Nafion SAC-13 (Sigma-Aldrich) was purchased and used directly. Sn-Beta (Si/Sn molar ratio of 400) was provided by Haldor Topsøe A/S, Denmark. Sulfonated carbon was synthesized according to the method reported by Takagaki et al.¹⁷ Amorphous SiO₂-Al₂O₃ was obtained from Grace Davison (SIAL 3113) and pretreated in air for 5 h at 823 K (1 K min⁻¹). NbOPO₄ was obtained from CBMM (Brazil) and used directly. Sulfuric acid (Fluka; 1.0 N) was used to prepare homogeneous catalyst solutions.

Temperature-Programmed Desorption of Ammonia. Temperature-programmed desorption of NH₃ was used to determine the total acid site density of each H-ZSM-5 zeolite (Figure S1). A quartz flow-through cell was loaded with 100 mg of H-ZSM-5. Before NH₃ adsorption, samples were pretreated

at 473 K for 1 h under flowing He (Airgas; industrial grade) at 100 cm³ (STP) min⁻¹ to remove adsorbed moisture. For NH₃ adsorption, 1 mol % NH₃ in He (Airgas) at 100 cm³ (STP) min⁻¹ was passed through the sample at 423 K for 45 min. Physisorbed NH₃ was removed by holding the sample at 423 K under flowing He at 100 cm³ (STP) min⁻¹ for 45 min. Temperature-programmed desorption was performed using a temperature ramp of 10 K min⁻¹ from room temperature to 973 K under flowing He at 50 cm³ (STP) min⁻¹. The desorbed NH₃ was quantified by an online mass spectrometer (OmniStar).

FTIR Spectroscopy of Adsorbed Pyridine. Infrared spectroscopy of adsorbed pyridine was used to determine the ratio of Brønsted to Lewis acid sites of the H-ZSM-5 zeolites (Figure S2). Approximately 20 mg of catalyst was placed into a die and pressed into a self-supporting pellet. Subsequently, the pellet was placed into a treatment/sampling cell where it was heated to 773 K under flowing He (Airgas; industrial grade) at 100 cm³ (STP) min⁻¹ for 1 h. An infrared spectrum of H-ZSM-5 was then taken to observe structural hydroxyl groups at an absorption band of 3745 cm⁻¹ (Figure S2).¹⁸ Pyridine (Sigma-Aldrich; anhydrous; 99.8%) was introduced into the cell through a bubbler for 30 min at room temperature. Physisorbed pyridine was removed by purging the cell with flowing He at 100 cm³ (STP) min⁻¹ for 2 h at 423 K, and then an infrared spectrum was taken. The areas of the pyridine peaks at 1455 and 1545 cm⁻¹ bands, assigned to Lewis and Brønsted acid sites, respectively,¹⁹ were determined by subtracting the spectra of the sample before and after pyridine exposure. The Brønsted/Lewis acid site ratios were obtained by normalizing the areas with integrated molar extinction coefficients reported in the literature: 1.67 cm² μmol⁻¹ for Brønsted sites and 2.22 cm² μmol⁻¹ for Lewis sites.¹⁹

Catalytic Activity Measurements. Furfuryl alcohol (Acros Organics; 98%), levulinic acid (Acros Organics; 98+%), tetrahydrofuran (Fisher; certified), γ -valerolactone (Sigma-Aldrich; 98+%), dimethyl sulfoxide (Sigma-Aldrich; ACS reagent; 99.9+%), 1,4-dioxane (Sigma-Aldrich; anhydrous; 99.8%), 1-methyl-2-pyrrolidone (Sigma-Aldrich; HPLC grade; 99+%), and acetonitrile (Sigma-Aldrich; 99.9+%) were used directly without further purification. For reaction studies (Figures 1-5), 1.5 mL of solution with the appropriate amounts of reactant, solvent, and catalyst were added in thick-walled

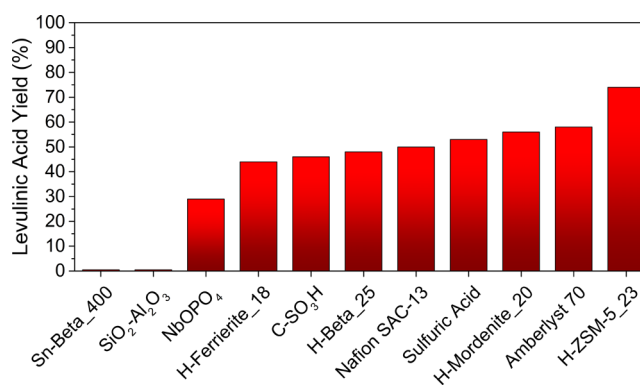


Figure 1. Maximum levulinic acid yields achieved for different acid catalysts. Reaction conditions: furfuryl alcohol (0.2 M), 4:1 THF-H₂O w/w solvent (1.5 mL), 393 K, and stirring at 700 rpm. Reactant to solid catalyst ratio (w/w) = 0.6. Sulfuric acid solution = 0.1 M. C-SO₃H refers to sulfonated carbon.

glass reactors (Alltech; 10 mL). The ratio of furfuryl alcohol to solid catalyst (w/w) was kept at 0.6, and 0.1 M sulfuric acid solutions were used unless otherwise noted. The reactors were placed in an oil bath at the desired reaction temperature and stirred at 700 rpm. Reactors were removed from the oil bath at specific reaction times and cooled by flowing compressed air. After reaction, the content of the reactor was filtered using a 0.2 μm membrane (VWR International; PTFE). Concentrations of furfuryl alcohol in liquid solution were quantified using a high-performance liquid chromatograph instrument (Waters Alliance 2695) equipped with a photodiode array detector (Waters 996) and a reversed-phase column (Agilent Technologies; Zorbax SB-C18; 4.6 \times 300 mm; 5 μm). A mobile phase of 5 mM sulfuric acid as the aqueous phase with acetonitrile as the organic modifier was used at a flow rate of 1.0 mL min^{-1} . Concentrations of levulinic acid in liquid solution were quantified using a high-performance liquid chromatograph (Waters Alliance 2695) instrument equipped with a differential refractometer (Waters 410), a photodiode array detector (Waters 996), and an ion-exclusion column (Bio-Rad; Aminex HPX-87H; 7.8 \times 300 mm, 5 μm). A mobile phase of 5 mM sulfuric acid at a flow rate of 0.6 mL min^{-1} was used. Reaction kinetics data (Table 1) were determined by the method of initial rates (Figure S3).

Table 1. Selectivity and Activity of H-ZSM-5 Zeolite with Various $\text{SiO}_2/\text{Al}_2\text{O}_3$ Ratios

catalyst	$\text{SiO}_2/\text{Al}_2\text{O}_3$	Bronsted acid site density ($\mu\text{mol g}^{-1}$)	Lewis acid site density ($\mu\text{mol g}^{-1}$)	maximum levulinic acid yield (%) ^a	furfuryl alcohol TOF (ks^{-1}) ^b
H-ZSM-5_23	23	650	28	74	7.0
H-ZSM-5_50	50	270	12	75	17
H-ZSM-5_80	80	210	10	75	23

^aReaction conditions: furfuryl alcohol (0.2 M), 4:1 THF–H₂O w/w solvent (1.5 mL), catalyst (50 mg), 393 K, and stirring at 700 rpm.

^bReaction conditions: furfuryl alcohol (0.18 M), 9:1 THF–H₂O w/w solvent (4 mL), catalyst (40 mg), 363 K, and stirring at 700 rpm.

RESULTS AND DISCUSSION

Figure 1 displays the maximum levulinic acid yields obtained using 0.2 M furfuryl alcohol in a 4:1 THF–H₂O w/w solvent system at 393 K using a range of acid catalysts with varying properties. Using sulfuric acid as the catalyst, moderate levulinic acid yields of 53% were achieved in 4:1 THF–H₂O, compared to yields of 23% when pure water was used as the solvent at the same reaction conditions. Accordingly, a 30% increase in the levulinic acid yield is obtained simply by performing the reaction in 4:1 THF–H₂O solvent compared with conversion in pure aqueous media.

The behavior of heterogeneous acid catalysts in polar aprotic solvents is not well studied, and thus, levulinic acid yields were measured for a variety of heterogeneous acid catalysts. For example, as shown in Figure 1, pure solid Brønsted acid catalysts, such as ion-exchanged resin Amberlyst 70, Nafion SAC-13, and sulfonated carbon (C–SO₃H), displayed similar levulinic acid yields (46–58%) relative to the homogeneous

sulfuric acid catalyst; however, pure solid Lewis acid catalysts, such as Sn-Beta_400 (Si/Sn molar ratio of 400), were not active for furfuryl alcohol conversion, suggesting that furfuryl alcohol hydrolysis/polymerization is catalyzed exclusively by Brønsted acids. Furthermore, zeolite H-Beta_25 (SiO₂/Al₂O₃ molar ratio of 25), which has a combination of Brønsted and Lewis acid sites, did not show a selectivity improvement for production of levulinic acid compared with pure Brønsted acid catalysts, unlike previous results for other biomass conversion reactions (e.g., arabinose conversion to furfural²⁰). Solid acid catalysts with predominately weak or moderate strength Brønsted acid sites resulted in low levulinic acid yields, suggesting that strong Brønsted acid catalysts are necessary for high levulinic acid yields. For example, NbOPO₄ achieved a 29% levulinic acid yield at complete furfuryl alcohol conversion, whereas amorphous SiO₂–Al₂O₃ was not active for the furfuryl alcohol conversion reaction.

The zeolite H-ZSM-5_23 (SiO₂/Al₂O₃ molar ratio of 23) displayed the highest levulinic acid yield of 74%, a yield increase of 15–30% relative to the measured values for the other acid catalysts, including zeolites, such as H-Ferrierite_18, H-Beta_25, and H-Mordenite_20 with similar SiO₂/Al₂O₃ molar ratios of 18, 25, and 20, respectively. Zeolite H-ZSM-5_23 contains a 3-dimensional channel system with medium size pore/cage diameters of ~ 5.5 Å,²¹ similar to the molecular dimensions of furfuryl alcohol. The larger pore/cage zeolites H-Beta_25 and H-Mordenite_20 (~ 0.7 and 0.6 Å, respectively), which have 3- and 1-dimensional channels, respectively, led to significantly lower levulinic acid yields (48% and 56%, respectively) compared with H-ZSM-5_23, suggesting that H-ZSM-5_23 has pore and cage dimensions large enough to allow furfuryl alcohol to diffuse through and convert to levulinic acid while significantly inhibiting the transition states for furfuryl alcohol polymerization reactions. Furthermore, H-Ferrierite_18, a 2-dimensional zeolite, which has smaller pore and cage dimensions of ~ 0.4 Å,²¹ showed the lowest levulinic acid yield of the range of zeolites, which can be attributed to significant furfuryl alcohol diffusion limitations through the zeolite channels, promoting furfuryl alcohol polymerization near the pore openings of H-Ferrierite_18.

The results from Figure 1 show that H-ZSM-5_23 is a highly selective catalyst. However, the major challenge of levulinic acid production from furfuryl alcohol is the high rate of furfuryl alcohol polymerization at high reactant concentrations. Thus, the effects of increasing furfuryl alcohol concentration on levulinic acid selectivity were explored (Figure 2). As the

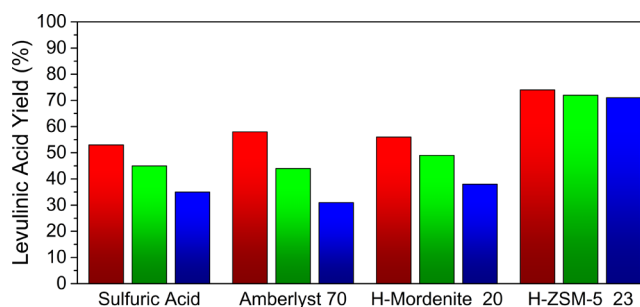


Figure 2. Maximum levulinic acid yields achieved at 0.2 M furfuryl alcohol (red), 0.5 M furfuryl alcohol (green), and 1 M furfuryl alcohol (blue). Reaction conditions: 4:1 THF–H₂O w/w solvent (1.5 mL), 393 K, and stirring at 700 rpm. Reactant to solid catalyst ratio (w/w) = 0.6. Sulfuric acid solution = 0.1 M.

furfuryl alcohol concentration was increased from 0.2 to 1 M, the levulinic acid yields at complete conversion using sulfuric acid, Amberlyst 70, and H-Mordenite_20 as catalysts decreased by ~20% as a result of the increasing extents of polymerization of furfuryl alcohol at higher reactant concentrations. Surprisingly, using H-ZSM-5_23, >70% levulinic acid yields are maintained up to 1 M furfuryl alcohol concentrations, showing that H-ZSM-5 zeolite has the ability to inhibit furfuryl alcohol polymerization, even at high reactant concentrations. This result is further evidence for shape selectivity effects of the H-ZSM-5_23 zeolite for furfuryl alcohol hydrolysis to levulinic acid.

In further experiments, we explored the effects of varying the water concentration on the hydrolysis of furfuryl alcohol to levulinic acid using H-ZSM-5_23 and sulfuric acid as catalysts with 1 M furfuryl alcohol at 393 K, as shown in Figure 3. When

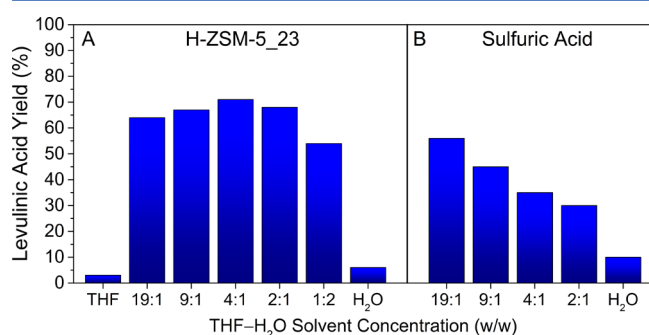


Figure 3. Maximum levulinic acid yields achieved at various THF-H₂O solvent concentrations using (A) H-ZSM-5_23 and (B) sulfuric acid as catalyst. Reaction conditions: furfuryl alcohol (1 M), solvent (1.5 mL), 393 K, and stirring at 700 rpm. Reactant to solid catalyst ratio (w/w) = 0.6. Sulfuric acid solution = 0.1 M.

the THF-H₂O solvent ratio was varied from 19:1 to 2:1 w/w using sulfuric acid as catalyst, the levulinic acid yields at complete conversion decreased with increasing water concentration (from 56% to 30%, in this example). However, when using H-ZSM-5_23 as the catalyst, levulinic acid yields remained nearly constant (64–71%) over the range of 19:1 to 2:1 THF-H₂O solvent, showing a maximum yield at 4:1 THF-H₂O solvent. Furthermore, with H-ZSM-5_23, moderate levulinic acid yields were maintained even when using low THF concentrations in the solvent system. For example, 54% levulinic acid yield was obtained in 1:2 THF-H₂O solvent using H-ZSM-5_23, whereas similar levulinic acid yields using sulfuric acid can be achieved only at high ratios of THF-H₂O solvent (e.g., 19:1).

The above results suggest that the internal solvent microenvironment in the H-ZSM-5 zeolite remains rather constant with varying concentrations of THF, even when low amounts of THF (i.e., 1:2 THF-H₂O) are present in the solvent system. It is well documented in the literature that the SiO₂/Al₂O₃ ratio in zeolites can alter the hydrophobicity/hydrophilicity of the zeolite.^{22,23} As the SiO₂/Al₂O₃ ratio increases, the zeolite becomes more hydrophobic. For example, siliceous zeolites, such as H-ZSM-5_23 are hydrophobic, whereas more aluminous zeolites have a strong affinity for water. Thus, the internal THF-H₂O solvent ratio within the zeolite framework can vary from the bulk THF-H₂O solvent ratio. In this case, a high THF-H₂O solvent ratio can be maintained within the internal H-ZSM-5_23 framework, even at low THF solvent

concentrations, because of the inherent hydrophobicity of H-ZSM-5_23, leading to constant levulinic acid yields over a wide range of THF-H₂O solvent ratios.

When using pure water as the solvent, low levulinic acid yields are achieved at complete conversion for both sulfuric acid and H-ZSM-5_23 (10% and 6%, respectively). This result indicates that high levulinic acid yields at high furfuryl alcohol concentrations using H-ZSM-5_23 are due to the synergistic effect of the structural properties of H-ZSM-5 as well as the increased reaction performance using the polar aprotic solvent THF. Finally, we carried out the reaction in pure THF using H-ZSM-5_23, resulting in 3% levulinic acid yield, and this result indicated the necessity of having a small fraction of water in the reaction system (i.e., water is a reactant for this reaction).

We have previously reported reactivity results for other acid-catalyzed biomass conversion reactions, obtaining increased reaction performance using polar aprotic solvents, such as γ -valerolactone (GVL) and THF, compared with reactions carried out in water using homogeneous acid catalysts.²⁴ Through reaction kinetics studies, we have determined that increased product yields are due to advantageous relative reaction rate increases in the presence of these polar aprotic solvents. For example, for the case of the acid-catalyzed dehydration of xylose to furfural, reaction rate increases of ~30 times were observed for furfural formation from xylose in GVL compared with the reaction carried out in water, whereas reaction rates of furfural resinification/degradation remained similar between the GVL and water solvent systems, leading to increased product yields in the polar aprotic solvent. From these previous results, we speculate that increased levulinic acid yields from furfuryl alcohol in THF-H₂O solvents are due to similar polar aprotic solvent effects.

Moreover, we have previously shown that the reaction rate for a hydrolysis reaction (i.e., cellobiose hydrolysis to glucose) exhibits an exponentially increasing trend with increasing concentrations of polar aprotic solvent composition in GVL-H₂O solvent mixtures.²⁵ Because the hydrophobicity of the zeolite may affect the internal solvent microenvironment within the zeolite, we studied the conversion of furfuryl alcohol in THF-H₂O solvents over H-ZSM-5 zeolites with varying SiO₂/Al₂O₃ ratios: H-ZSM-5_23, H-ZSM-5_50, and H-ZSM-5_80 (SiO₂/Al₂O₃ molar ratios of 23, 50, and 80, respectively). The results are displayed in Table 1. Levulinic acid yields of ~75% were achieved for all three H-ZSM-5 zeolites in 4:1 THF-H₂O solvent at 393 K, which suggests that the internal THF-H₂O solvent microenvironment within the structure remained similar for all three H-ZSM-5 catalysts, despite changing the SiO₂/Al₂O₃ ratio.

The above result can be attributed to lattice defects in the zeolite framework, which can cause residual hydrophilicity. IR spectra of each H-ZSM-5 confirmed the presence of defect hydroxyl groups (Figure S2; 3745 cm⁻¹ band),¹⁸ and this hydroxyl absorption band increases in intensity with increasing SiO₂/Al₂O₃ ratio (i.e., SiO₂/Al₂O₃ = 23, 50, and 80, respectively), which can allow for a similar solvent microenvironment within these ZSM-5 zeolites. Furthermore, a previous study regarding the separation of THF-H₂O mixtures using zeolite membranes showed that the THF-H₂O separation selectivity remained on the same order of magnitude for zeolites with SiO₂/Al₂O₃ molar ratios >20.²⁶

A similar solvent microenvironment allows for the comparison of reaction kinetics using these H-ZSM-5 catalysts with varying SiO₂/Al₂O₃ ratios. Turnover frequencies (TOF) of

furfuryl alcohol conversion for each H-ZSM-5 zeolite were measured using the method of initial rates (Figure S3) with 0.18 M furfuryl alcohol in 9:1 THF–H₂O at 363 K (Table 1). Interestingly, the TOF values increased with decreasing acid site density (increasing SiO₂/Al₂O₃ ratio) of H-ZSM-5. According to Madon and Boudart,²⁷ a TOF dependence on the number of active sites indicates internal mass transfer limitations, suggesting that the catalytic activity of H-ZSM-5 is governed by the mass transfer of furfuryl alcohol into the zeolite framework. The presence of diffusion limitations in the conversion of furfuryl alcohol using H-ZSM-5 further supports the suggestion that the internal pore size and structure of H-ZSM-5 are important for achieving high yields in the hydrolysis of furfural: the pore size is sufficiently large to allow furfuryl alcohol to diffuse in, maintaining low concentrations of furfuryl alcohol near the acid sites, and the cage size is sufficiently large to allow furfuryl alcohol to hydrolyze to levulinic acid while inhibiting transition states involved in furfuryl alcohol polymerization reactions due to shape selectivity effects.

More generally, we have found that increased levulinic acid yields from furfuryl alcohol can also be obtained using other aprotic solvents. Figure 4 displays the maximum levulinic acid

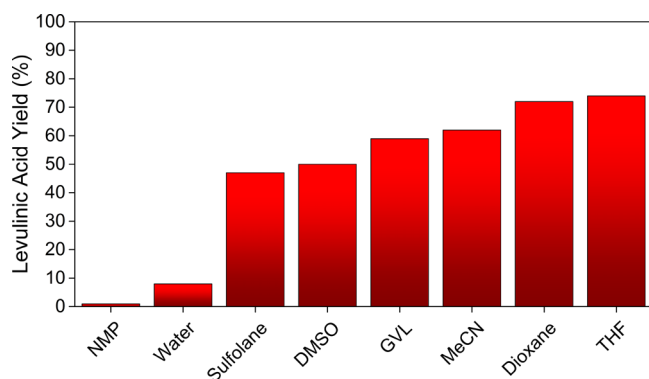


Figure 4. Maximum levulinic acid yields achieved with various aprotic solvent–water mixtures using H-ZSM-5_23 as catalyst. Aprotic solvent mixtures contained 10 M water. Reaction conditions: furfuryl alcohol (0.25 M), solvent (1.5 mL), catalyst (50 mg), 393 K, and stirring at 700 rpm.

yields achieved at complete conversion for a range of aprotic solvent–water systems with 0.25 M furfuryl alcohol and 10 M water using H-ZSM-5_23 as catalyst at 393 K. Similar to using THF as a solvent, levulinic acid yields greater than 70% can be achieved using dioxane solvent systems compared with 6% levulinic acid yield obtained using pure aqueous solution. Furthermore, 60% levulinic acid yields were achieved using acetonitrile (MeCN) and GVL solvent systems, and the use of dimethyl sulfoxide (DMSO)– and sulfolane–water solvents resulted in 50% levulinic acid yields. Moreover, furfuryl alcohol remained unconverted with *N*-methylpyrrolidone (NMP)–water solvent due to acid-site poisoning of H-ZSM-5 from the Lewis basicity of NMP. Therefore, these aprotic solvent effects are not limited to THF, and this effect is of general significance.

We have addressed the stability of ZSM-5 catalysts for the conversion of furfuryl alcohol to levulinic acid by conducting successive cycles of reaction followed by reutilization using H-ZSM-5_23 with 1 M furfuryl alcohol in 4:1 THF–H₂O at 393 K for 0.5 h. The results are shown in Figure 5. After a single cycle, the levulinic acid yield decreased by more than half, from 74% to 34%, because of the formation of surface humins

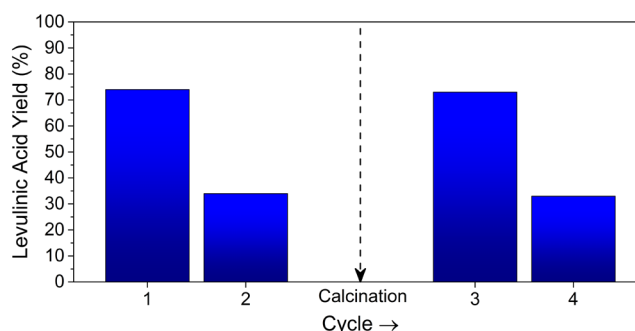


Figure 5. H-ZSM-5_23 catalyst recycling study. Maximum levulinic acid yields achieved at complete furfuryl alcohol conversion. Calcination performed between cycles 2 and 3. Reaction conditions: furfuryl alcohol (1 M), 4:1 THF–H₂O w/w solvent (1.5 mL), 393 K, 0.5 h, and stirring at 700 rpm. Reactant-to-solid catalyst ratio (w/w) = 0.6.

(carbonaceous residues) on the catalyst. However, zeolites have high thermal and chemical stability, allowing for high-temperature calcination treatments that would otherwise degrade organic-based acidic materials/supports.²⁸ After calcination of H-ZSM-5 at 823 K for 5 h between reaction cycles 2 and 3, a levulinic acid yield of 73% was obtained on the third cycle as a result of the removal of surface humins, indicating that the original levulinic acid yield can be recovered upon calcination.

The aforementioned results give insights into rational catalyst design for furfuryl alcohol hydrolysis to levulinic acid at high reactant concentrations. For example, a hydrophobic material that maintains low water concentrations within the internal catalyst structure, combined with a diffusion barrier to eliminate high furfuryl alcohol concentrations near the acid sites could be a favorable catalyst template for the furfuryl alcohol conversion reaction into levulinic acid as well as other acid-catalyzed reactions. Furthermore, the H-ZSM-5/THF reaction system can be further optimized for levulinic acid production from furfuryl alcohol. For instance, it is well-known in the literature that furfuryl alcohol polymerization reactions are promoted at higher temperatures.¹⁵ Thus, we have performed the furfuryl alcohol hydrolysis to levulinic acid reaction at 353 K with 0.2 M furfuryl alcohol in 4:1 THF–H₂O w/w solvent, achieving an 81% levulinic acid yield using H-ZSM-5_23 as catalyst. This result is a slight improvement from the 74% levulinic acid yield achieved at 393 K using H-ZSM-5_23 at the same experimental conditions (i.e., Figure 1); however, the catalytic activity was significantly decreased at lower temperature.

CONCLUSIONS

In summary, we have demonstrated that monophasic THF–H₂O solvent systems can be used to obtain high levulinic acid yields (>70%) with furfuryl alcohol solutions in high concentration (1 M) using H-ZSM-5 as catalyst. The zeolite H-ZSM-5_23 (SiO₂/Al₂O₃ molar ratio of 23) maintained high product selectivity over a wide range THF–H₂O solvent concentrations (>1:2 THF–H₂O w/w), in contrast to the homogeneous sulfuric acid catalyst, which is due to the hydrophobic nature of the zeolite. Furthermore, through comparison of reaction performance with structurally similar zeolites (e.g., H-Beta, H-Mordenite, and H-Ferrierite), combined with the observation of possible internal mass transport limitations, we suggest that H-ZSM-5 zeolite has

structural dimensions that are effective for furfuryl alcohol hydrolysis to levulinic acid, while inhibiting furfuryl alcohol polymerization to degradation products. These structural effects of H-ZSM-5 combined with the increased reaction performance using the polar aprotic solvent THF lead to high levulinic acid yields at high furfuryl alcohol concentrations.

■ ASSOCIATED CONTENT

● Supporting Information

The Supporting Information is available free of charge on the ACS Publications website at DOI: 10.1021/acscatal.5b00274.

TPD profiles, FTIR spectra, and reaction kinetics data (PDF)

■ AUTHOR INFORMATION

Corresponding Author

*E-mail: jdumesic@wisc.edu.

Notes

The authors declare no competing financial interest.

■ ACKNOWLEDGMENTS

This work was supported in part by the U.S. Department of Energy, Office of Basic Energy Sciences and by the DOE Great Lakes Bioenergy Research Center (<http://www.glbrc.org>), which is supported by the U.S. Department of Energy, Office of Science, Office of Biological and Environmental Research, through the Cooperative Agreement BER DE-FC02-07ER64494 between The Board of Regents of the University of Wisconsin System and the U.S. Department of Energy. D.M.A. acknowledges financial support from Glucan Biorenewables, LLC. We acknowledge Jiayao Chen, Claire Johnson, and Nathan Prisco for help with experiments, and we thank Helen Luo and Professor Yuriy Román-Leshkov for valuable discussions.

■ REFERENCES

- (1) Werpy, T. A.; Holladay, J. E.; White, J. F., *Top Value Added Chemicals from Biomass: I. Results of Screening for Potential Candidates from Sugars and Synthesis Gas*, PNNL-14808; Pacific Northwest National Laboratory: Richland, WA, 2004.
- (2) Bozell, J. J.; Petersen, G. R. *Green Chem.* **2010**, *12*, 539–554.
- (3) Bozell, J. J.; Moens, L.; Elliott, D. C.; Wang, Y.; Neuenschwander, G. G.; Fitzpatrick, S. W.; Bilski, R. J.; Jarnefeld, J. L. *Resour., Conserv. Recycl.* **2000**, *28*, 227–239.
- (4) Elliott, D. C.; Frye, J. G. U.S. Patent US5883266A, 1999.
- (5) Lake, M. A.; Burton, S. W.; Fuller, W. C.; Sasser, R.; Lindstrom, M. E.; Wheless, J. T. U.S. Patent US20100312006A1, 2010.
- (6) Demolis, A.; Essayem, N.; Rataboul, F. *ACS Sustainable Chem. Eng.* **2014**, *2*, 1338–1352.
- (7) Manzer, L. E. U.S. Patent US6617464B2, 2003.
- (8) Chia, M.; Dumesic, J. A. *Chem. Commun.* **2011**, *47*, 12233–12235.
- (9) Hayes, D. J.; Fitzpatrick, S.; Hayes, M. H. B.; Ross, J. R. H. In *Biorefineries – Industrial Processes and Products*; Wiley-VCH Verlag GmbH: Weinheim, 2008; pp 139–164.
- (10) Farone, W. A.; Cuzens, J. E. U.S. Patent US6054611A, 2000.
- (11) Balat, M.; Balat, H.; Oz, C. *Prog. Energy Combust. Sci.* **2008**, *34*, 551–573.
- (12) Gurbuz, E. I.; Wettstein, S. G.; Dumesic, J. A. *ChemSusChem* **2012**, *5*, 383–387.
- (13) Wettstein, S. G.; Alonso, D. M.; Gürbüz, E. I.; Dumesic, J. A. *Curr. Opin. Chem. Eng.* **2012**, *1*, 218–224.
- (14) González-Maldonado, G. M.; Assary, R. S.; Dumesic, J.; Curtiss, L. A. *Energy Environ. Sci.* **2012**, *5*, 6981–6989.

- (15) Kim, T.; Assary, R. S.; Marshall, C. L.; Gosztola, D. J.; Curtiss, L. A.; Stair, P. C. *ChemCatChem* **2011**, *3*, 1451–1458.
- (16) Lange, J. P.; van de Graaf, W. D.; Haan, R. J. *ChemSusChem* **2009**, *2*, 437–441.
- (17) Takagaki, A.; Toda, M.; Okamura, M.; Kondo, J. N.; Hayashi, S.; Domen, K.; Hara, M. *Catal. Today* **2006**, *116*, 157–161.
- (18) Emeis, C. A. J. *Catal.* **1993**, *141*, 347–354.
- (19) Qin, G. L.; Zheng, L.; Xie, Y. M.; Wu, C. C. *J. Catal.* **1985**, *95*, 609–612.
- (20) Gallo, J. M. R.; Alonso, D. M.; Mellmer, M. A.; Yeap, J. H.; Wong, H. C.; Dumesic, J. A. *Top. Catal.* **2013**, *56*, 1775–1781.
- (21) Baerlocher, Ch.; McCusker, L. B. *Database of Zeolite Structures*; <http://www.iza-structure.org/databases/>.
- (22) Chen, N. Y. J. *Phys. Chem.* **1976**, *80*, 60–64.
- (23) Taguchi, A.; Schuth, F. *Microporous Mesoporous Mater.* **2005**, *77*, 1–45.
- (24) Mellmer, M. A.; Sener, C.; Gallo, J. M. R.; Luterbacher, J. S.; Alonso, D. M.; Dumesic, J. A. *Angew. Chem., Int. Ed.* **2014**, *53* (44), 11872–11875; *Angew. Chem.* **2014**, *126*, 12066–12069.
- (25) Mellmer, M. A.; Alonso, D. M.; Luterbacher, J. S.; Gallo, J. M. R.; Dumesic, J. A. *Green Chem.* **2014**, *16*, 4659–4662.
- (26) Li, S. G.; Tuan, V. A.; Noble, R. D.; Falconer, J. L. *Ind. Eng. Chem. Res.* **2001**, *40*, 4577–4585.
- (27) Madon, R. J.; Boudart, M. *Ind. Eng. Chem. Fundam.* **1982**, *21*, 438–447.
- (28) Petrovic, I.; Navrotsky, A.; Davis, M. E.; Zones, S. I. *Chem. Mater.* **1993**, *5*, 1805–1813.